Development of Electrostrictive Force-Feeding Sub-system for Liquid Pulsed Plasma Thrusters

IEPC-2019-931

Presented at the 36th International Electric Propulsion Conference
University of Vienna, Austria
September 15-20, 2019

Cristian Dobranszki,* Igor O. Golosnoy† and Stephen B. Gabriel‡
University of Southampton, Southampton, Hampshire, SO17 1BJ, United Kingdom

and

Paolo Gessini,§
University of Brasilia, Gama Campus, Brasilia, DF, 72444-240, Brazil

Abstract: An electrostatically driven pressure valve has been successfully developed based on the *electrostrictive force*, delivering propellant to the discharge chamber via an open-end conduit, free of any moving parts. The proof-of-concept unit has been built and demonstrated stable operation. It was shown that the conventional theory of electrostriction in liquid dielectrics is applicable for the device. The electrostatic pump has been designed for a coaxial liquid-fed micro pulsed plasma thruster prototype operating in the 1 - 2 J energy range. Active mass dosage capability is proven as a function of applied voltage and pump operational time, introducing a new class of electronically controlled feeding systems. Experimental measurements demonstrate a minimum achievable mass bit ranging from 77 to 164 μg using the voltage-controlled operation. Moreover, the pump is able to deliver up to 1 mg of propellant for a single shot. In addition to the active control, the mass flow rate can be passively adjusted by changing the capillary dimensions (radius and length), conduit material and the propellant dielectric properties.

Nomenclature

I_{sp}	= Specific Impulse
f	= Force density
σ_f	= Free charge
E	= Electric field
ρ	= Liquid (propellant) density
ε	= Dielectric Permittivity $\varepsilon = \varepsilon_0 \varepsilon_r$
ε_0	= Permittivity of free space $\varepsilon_0 \simeq 8.854 \times 10^{-12}$ F $\cdot$ m^{-1}
ε_r	= Relative permittivity of the liquid (propellant)
T	= Temperature
v_{PFPE}	= Velocity of PFPE
p	= Pressure
p_{EST}	= Electrostrictive pressure component

*Doctoral Candidate, Electrical Power Engineering Research Group, ECS, C.Dobranszki@soton.ac.uk
†Associate Professor, Electrical Power Engineering Research Group, ECS, I.Golosnoy@soton.ac.uk
‡Professor, Electrical Power Engineering Research Group, ECS, sbg2@soton.ac.uk
§Associate Professor, Aerospace Engineering, University of Brasilia, paolo.gessini@aerospace.unb.br

p_{cap} = Capillary pressure (Young-Laplace equation)
p_{hs} = Hydrostatic pressure
p_{atm} = Atmospheric pressure
Δp = Pressure difference between two points
h = Height due to capillary rise
L_c = Length of the feeding conduit
r_c = Radius of the feeding conduit
Q = Volumetric flow rate $\left(\frac{\dot{m}}{\rho}\right)$
$\dot{z}$ = Velocity of liquid along the z-axis
A = Cross-sectional area of conduit ($A = \pi\, r_c^2$)
ν = Viscosity (kinematic)
t_{asc} = Ascending time of liquid droplet
t_{spr} = Spreading time of liquid droplet (over the thruster back-wall)
t_{op} = Operational time of the electrostatic valve
$\dot{m}$ = Mass flow rate
m_{bit} = Mass bit
V_{tank} = Volume of propellant in tank
I_{bit} = Impulse bit
E_{shot} = Discharge energy per pulse

I. Introduction

THE space industry interest in ever-smaller satellites is growing worldwide.[1,2] Although debatable if an economic advantage can be expected from an electric propelled or a natural drag de-orbiting small satellite, the debate typically settles on a sufficiently reliable and economically beneficial propulsion system. The appeal of Pulsed Plasma Thrusters (PPTs) to the present market trend is hindered by apparent shortcomings in terms of efficiency, and lifetime limiting factors such as Late-Time Ablation (LTA) effects and charring deposition. Nevertheless, PPTs are a mature technology with proven in-flight reliability, low implementation cost and simple operation. Their versatile scalability, robustness and compact-built recommends them for satellite applications in the CubeSat range.[1]

Traditional Solid-fed PPTs (SPPTs) comprise several chained processes within one operational cycle, which cannot be discretely analyzed. Typically, a capacitor is charged to a set voltage, holding the potential over the anode and cathode until a spark plug initiates the discharge, and consequently the thrust. It has been established that the thrust in PPTs is generated by two different mechanisms.[3] The plasma produced in the discharge conducts the current, which in turn results in electromagnetic acceleration by the Lorentz force; the charged species are accelerated to speeds exceeding 40 km/s.[4,5] During the discharge the plasma heats and vaporizes propellant leading to the second acceleration mechanism - gas-dynamic expansion of the exhaust. The gas-dynamic forces accelerate the remaining gas-plasma vapour to speeds much below 3 km/s,[4] the average exhaust velocity. Although both components of the thrust must co-exist in any PPT, clearly, the gas-dynamic component must be minimized to allow high I_{sp} and higher overall efficiency. The main consequence of thermodynamic component is known to be the Late-Time Ablation (LTA) effect, vaporization of the propellant after the discharge takes place. This is primarily responsible for the low efficiency, and limited I_{sp} capabilities of the device.[6]

It is almost impossible to reduce late-time ablation in SPPTs. The spring feeding system employed in traditional Solid-fed PPTs (SPPTs) preserves the simplicity and reliability of the device. However, it forces the propellant bar to remain in contact with the plasma sheet which heats the Teflon surface to sublimating temperatures for as long as 100 μs after the pulse finalizes, accounting for 40% of the ablated mass bit which is not electromagnetically accelerated.[7] Notable efforts have been done towards decreasing LTA effects, via High Frequency Burst (HFB) operation[8] and Two-Stage PPT (TS-PPT) operation[9] for PTFE propelled thrusters, however, pulse-forming networks are required for this operational mode. A different approach to solving the excessive neutral vapour problem is selective dosing of the fuel via an active feeding system and optimizing the ratio of mass bit to discharge energy - as such, the usable electrical energy can rapidly sublimate the

discrete mass bit, and sufficient energy remains available to ionize and electromagnetically accelerate the propellant. Moreover, since the heat injection during a single shot acts only on the discretized mass bit, LTA would be significantly reduced, or eliminated. Active feeding systems such as injectors/syringes,[10–12] MEMS pumps[13] and solenoid valves[14] have been used in experimental Liquid-fed PPTs (LPPTs), however, they compromise the reliability and simplicity of traditional PPT. Additionally, they would increase the power requirements of the thruster which is unavailable within the tight power budget of a nano-satellite. A Passive Flow Control (PFC) unit with porous feeder has been tested with water[15] and PFPE[16] that satisfies most requirements of a simple and economical PPT. Nonetheless the PFC unit has its main drawbacks regarding the uncontrolled mass bit ablation and LTA effects. Consequently, an active feeding unit of low power consumption and no moving parts is required to open the avenue of development and market appeal for liquid-fed micro pulsed plasma thrusters.

Preserving the robust operation of PPTs implies no moving parts and hence a liquid propellant must replace the solid propellant if active feeding is targeted. Therefore, PFPE is employed in this study to demonstrate the feasibility of a purely electrostatic feeding unit, which can actively control and deliver propellant to the discharge chamber. The proposed Electrostrictive Force-Feeding (EFF) unit employs a diverging electric field that moves the liquid from the tank to the thruster chamber, wetting the surface of the thruster back-wall, representative of breech-fed thruster operation. At the initial stages of the experimental work, an idealized point-to-plane electrode geometry was used over a height of 10 mm, generating a pressure in excess of 450 Pa, this repeatedly "lifted" the liquid against gravity. However, it must be noted that in the feeding unit designed to incorporate a traditional LPPT, an idealized point-to-plane geometry is not readily achievable and an approximation is thus employed to maintain manufacturing simplicity. The operation of the EFF pump is demonstrated using the non-idealized case of electrode geometry, which deviates from a point-to-plane electric field distribution, achieving pressures in excess of 150 Pa.

This article will address the fundamental physical principles of forces developed in liquid dielectrics and how they can generate pressure gradients that lead to a novel propellant delivery method. The calculated pressure is then used to model laminar flow conditions and to help design a feeding unit that can reliably output a mass bit in the range of 100-200 micrograms, for the proof-of-concept stage. The test cell and methodology build based on the calculation are briefly discussed to give a better understanding of the experimental results. Mass bit measurements obtained using the developed EFF pump are then presented and discussed. Finally, the future direction of this work is given.

II. Theoretical Considerations and Modelling

A. Electrical Forces in Dielectric Liquids

Dielectric liquids stressed by strong electric fields will develop a pressure gradient due to the dipole moment induced by the applied field. The electrostatic problem is coupled with the fluid dynamics and the liquid motion is manipulated via capillary geometries to achieve propellant delivery in the microgram range, applicable to electric propulsion devices. The fundamental phenomena governing the pumping effect has been theoretically predicted in 1880 by Korteweg,[17] developed by Helmholtz in 1881[18] and experimentally tested as early as 1895 by Pellat.[19] Equation (1)[17] describes the electrical body forces arising in a dielectric liquid, where σ_f, E, ε and ρ represent the free charge inside the bulk material, applied electric field, liquid permittivity and density, respectively.

$$\boldsymbol{f} = \sigma_f \boldsymbol{E} - \frac{1}{2}E^2\nabla\varepsilon + \frac{1}{2}\nabla\left[E^2\rho\left(\frac{\partial\varepsilon}{\partial\rho}\right)_T\right] \tag{1}$$

The terms in Eq. (1) describe respectively the *electrostatic force density* due to the presence of free (or injected) charges inside the dielectric. The *dielectrophoretic force density* generated by inhomogeneities in the dielectric medium (which can arise due to temperature or pressure variations). And lastly, the *electrostrictive force density* due to non-uniformity of the electric field; in this system is the last term that generates the "pumping force", and presumably that requires to be maximized when designing an EFF pump.

The force density in Eq. (1) can be expressed as the gradient of (electric) pressure ∇p. This suggests that a valve-less feeding sub-system with no moving parts is feasible if the electrostatic field can be employed to "pump" the propellant into the discharge chamber. Considering the case of an isotropic dielectric media

($\nabla\varepsilon = 0$), where no free charge is present or introduced ($\sigma_f = 0$), Eq. (1) reduces to the following form:

$$\boldsymbol{f} = \frac{1}{2}\nabla\left[E^2\rho\left(\frac{\partial\varepsilon}{\partial\rho}\right)_T\right] \tag{2}$$

The pressure inside the liquid must attain equilibrium after an electric field is established inside the dielectric medium. Thus, force balance yields Eq. (3):

$$\nabla\mathbf{p} = \boldsymbol{f} = \frac{1}{2}\nabla\left[E^2\rho\left(\frac{\partial\varepsilon}{\partial\rho}\right)_T\right] \tag{3}$$

Considering two arbitrary points inside the dielectric fluid, where z_1 resides inside the non-uniform electric field and z_2 resides outside the non-uniform electric field, for an incompressible fluid (i.e. $\nabla\rho = 0$), Eq. (3) can be written in integral form as per Eq. (4)[17]:

$$\int_{z_1}^{z_2} dp = \frac{1}{2}\,\rho\,\varepsilon_0\left[E^2\left(\frac{\partial\varepsilon}{\partial\rho}\right)_T\right]_{z_1}^{z_2} \tag{4}$$

Applying the Clausius-Mossotti function[20] given by Eq. (5), relates the dielectric permittivity and density of a non-polar liquid, to Eq. (4) yields Eq. (6), allowing a simplification of the theoretical treatment

$$\rho\,\frac{\partial\varepsilon}{\partial\rho} = \frac{1}{3}(\varepsilon_r + 2)(\varepsilon_r - 1) \tag{5}$$

$$\Delta p = \frac{1}{2}\,\varepsilon_0\,(E_{z_2} - E_{z_1})^2\left[\frac{(\varepsilon_r + 2)(\varepsilon_r - 1)}{3}\right] \tag{6}$$

where E_{z_2} and E_{z_1} denote the electric field magnitude at the pressure points p_2 and p_1, respectively. In most practical applications the electric field E_{z_2} becomes zero (due to the electrode positioning and conduit geometry) and the final form of the pressure equation is then given by Eq. (7):

$$\Delta p = \frac{1}{2}\,\varepsilon_0\,{E_{z_1}}^2\left[\frac{(\varepsilon_r + 2)(\varepsilon_r - 1)}{3}\right] \tag{7}$$

Equation (7) is a formulation of pressure difference within the liquid dielectrics, where the electrostrictive force attracts the dipoles towards the region of highest electric field density, consequently building a local pressure inside the dielectric liquid. If coupled with specific flow geometries, an EFF unit can be designed.

B. Pressure Determination

The velocity of PFPE due to diverging electric fields, moving in a direction such that it opposes gravity, has been previously measured to be $v_{PFPE} = 0.242 \pm 0.010$ m·s^{-1}.[21] Using this velocity the Reynolds number characterizing the feeding system is 2.63, hence sufficiently low to assume laminar flow and employ the Hagen-Poiseuille model.[22]

The pressure inside the conduit can be computed by accounting for all pressure terms contributing to the system at a given point (i.e. electrostrictive, capillary, hydrostatic and atmospheric), the general formula is given by Eq. (8)

$$p = p_{EST} + p_{cap} + p_{hs} - p_{atm} \tag{8}$$

and taking the pressure difference at $z_1 = h$ and at $z_2 = L_c$ (see Fig. (1)) yields Eq. (10)

$$\Delta p = \left(p_{EST} + p_{cap} + p_{hs} - p_{atm}\right)\Big|_{z=h} - \left(p_{EST} + p_{cap} + p_{hs} - p_{atm}\right)\Big|_{z=L_c} \tag{9}$$

$$= p_{EST}\Big|_{z=h} - p_{hs}\Big|_{z=L_c} = \frac{1}{2}\,\varepsilon_0\,{E_h}^2\left[\frac{(\varepsilon_r + 2)(\varepsilon_r - 1)}{3}\right] - \rho\,g\,(L_c - h) \tag{10}$$

where E_h denotes the electric field strength at position h (see Fig. (1)), h is the liquid height due to capillary effects and L_c is the length of the conduit.

C. Fluid Flow Model

A laminar flow calculation, based on the Hagen-Poiseuille model, is used to relate the mass bit to the applied voltage and time parameter. The pressure induced by an applied electric field is estimated from Eq. (10). The Hagen-Poiseuille equation[22] is employed to relate the volumetric flow rate of the liquid to a given pressure drop, as per Eq. (11)

$$Q = \frac{1}{8}\frac{\pi\, {r_c}^4}{\nu\, \rho\, z}\, \Delta p \tag{11}$$

where Q is the volumetric flow rate of liquid (inside the conduit), Δp is the pressure drop across the points of interest, r_c is the conduit radius, z is the length between the pressure drop points, ν and ρ are the kinematic viscosity and density of the liquid, respectively.

If the volumetric flow rate is expressed as $Q = \dot{z} \cdot A$, an average velocity of the liquid can be computed.[22] Thus, re-arranging Eq. (11) yields the ascending time of the liquid, given by Eq. (12), which defines the time required for the liquid to reach the top of the feeding line, and hence the discharge chamber, after the voltage is engaged.

$$t_{asc} = \frac{4\,\nu\,\rho}{\Delta p}\left(\frac{(L_c - h)}{r_c}\right)^2 \tag{12}$$

here L_c is the conduit length and h is the capillary rise inside the conduit.

The Hagen-Poiseuille equation can be used inside the conduit domain to predict the value of t_{asc}. Once the liquid reaches the top of the conduit, it will spread over the back-wall of the discharge chamber, where the simple laminar flow model cannot be used to account for the droplet mass.

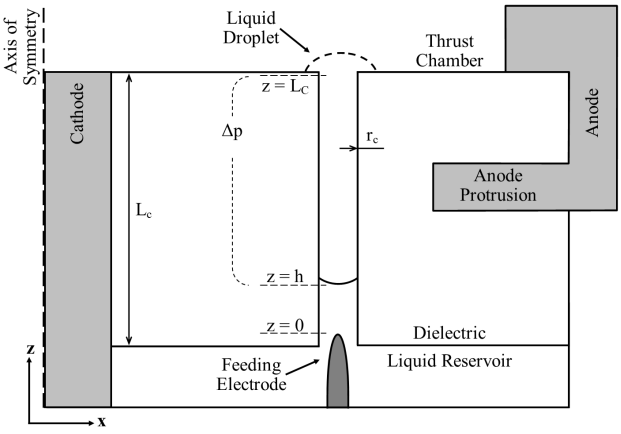

Figure 1. Fluid flow model schematic representing the operational mechanism of the EFF pump. L_c is the length of the conduit (feeding line), h is the height due to capillary effects and r_c is the conduit radius.

The fluid model can be extrapolated to obtain an upper limit of the mass bit if the flow rate of the liquid inside the column is considered, where the substitution $Q = \frac{\dot{m}}{\rho}$ is made in Eq. (11), yielding:

$$m_{bit} = \frac{1}{8}\frac{\pi\, {r_c}^4}{\nu\, L_c}\, \Delta p\; t_{spr} \tag{13}$$

where t_{spr} denotes the time required for the liquid to spread over the open surface (thruster back-wall).

Evidently, the liquid must rise prior to spreading; by convention the delivered mass bit is zero during the ascending time. From an experimental viewpoint, the ascending time and spreading time determine the duration that voltage must be engaged to deliver a specific mass bit, hence the operational time (t_{op}) of the electrostatic pump.

III. Experimental Design, Circuitry and Methodology

A. Test Cell Design

An EFF test cell has been manufactured in-house, based on a specific design geometry that enhances the fluid flow at selected pressure gradients. A plastic unit ensures the liquid propellant and electrical connections are held in place. The ceramic component that embodies the feeding conduit is placed at the top of the plastic unit, such that the liquid resides at the base of the feeding conduit and the discharge chamber is at the top of the feeding conduit, as per Fig. (2). Two electrodes are fixed in place by the plastic unit and ceramic component, they generate the diverging electric field inside the fluidic line.

The EFF unit is integrated in a coaxial micro-PPT prototype to obtain a more comprehensive understanding of the feeding unit feasibility in a realistic test cell, where all electric fields specific to a PPT operation are applied (spark plug, anode-cathode and EFF unit). The integrated design, as depicted in Fig. (2), is used for all reported measurements and will be employed for PPT diagnostics once the EFF unit is further optimised.

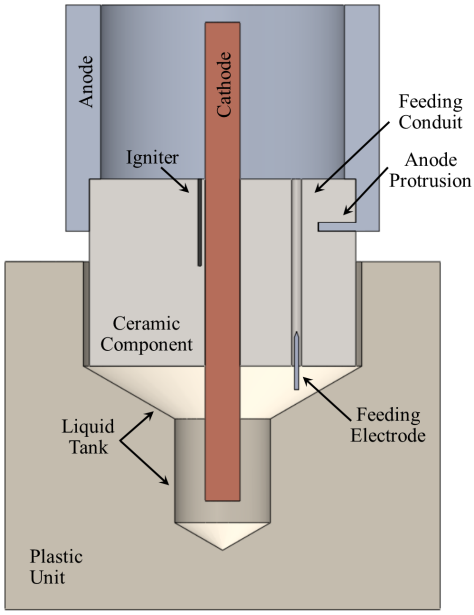

Figure 2. Schematic test cell of the electrostrictive force-feeding unit inside a coaxial LPPT prototype.

The propellant of choice for this coaxial micro-thruster is PFPE, due to its low vapour pressure, dielectric constant, optimal viscosity and similar PPT performance to Teflon.[16] From Fig. (2) it can be seen that the feeding unit has no moving parts, and it will be demonstrated later that it offers active propellant delivery. Implementing the EFF unit preserves the simplicity of the device; it is cost effective and robust due to its intrinsically fundamental operational mechanism. Moreover, all components are manufactured from standard vacuum-proof materials. Two main drawbacks have been identified for this design; firstly, the feeding electrode requires an additional voltage signal, and secondly, a time delay is introduced as propellant travels through the conduit. The former issue can be solved by employing voltage dividers and making use of the already existing high-voltage (HV) signals. The latter issue is intrinsic for any thruster where the propellant is not located in the discharge chamber permanently; however, the advantage implied by this feeding method targets a significant reduction or elimination of the LTA effects, and thus a beneficial trade-off between higher I_{sp} and lower operational frequency of the PPT.

B. Circuitry and Methodology

To operate the EFF unit a standard HV power supply is employed, characterized by low ripple, with a voltage rise time in the range of 61.83 ± 1.12 ms. The power supply is used to bias the feeding electrode, while the protruding electrode is at anode potential. This generates the high electric field required for the electrostrictive force to dominate the gravitational force. The cathode is grounded and the spark plug is operated via a dedicated HV power supply.

Once the test cell is cleaned, the propellant is added and the test cell closed using the ceramic component. The maximum amount of liquid in the tank is $V_{tank} = 0.49$ g. The voltage is then applied to the electrodes allowing the droplet to ascend into the discharge chamber. The voltage ramp rate is consistent throughout all experiments to warrant the dipole moment does not respond differently between experimental trials, this is an important parameter that must be carefully considered in all circuit designs.

Mass measurements are acquired using a non-intrusive video-graphic method. The liquid droplet rising into the discharge chamber is recorded, and the footage analyzed frame-by-frame. The frame containing the largest droplet is calibrated, and the droplet height and base radius are measured to compute the volume of the spherical cap (deviations from spherical symmetry are negligible and hence disregarded in the error

analysis). Using the propellant density the mass is computed, this is reported as the mass bit in the results section. The video-graphic method offers time resolution of 0.034 s and reliable spatial resolution down to 50 μm, corresponding to a mass bit of 18.41 μg.

In terms of the error analysis, five measurements are done for each variable (height and base radius) on each frame, where the standard deviation value is considered. Each data point represents the average of five measurements at the same condition; the standard deviation and instrumental error are used to generate the final uncertainty. The instrumental uncertainty associated with the voltage is negligible.

C. Experimental Results

Experimental results of the EFF unit with PFPE as propellant have been obtained for three different electric fields by varying only the applied voltage. Additionally, the operational time, t_{op} is varied to better understand the limitations of the feeding unit.

Each electric field value has an associated liquid ascending time, t_{asc}, corresponding to zero mass bit; they are represented on the plot of Fig. (3) by the hollow data point markers on the x-axis (t_{asc} at E).

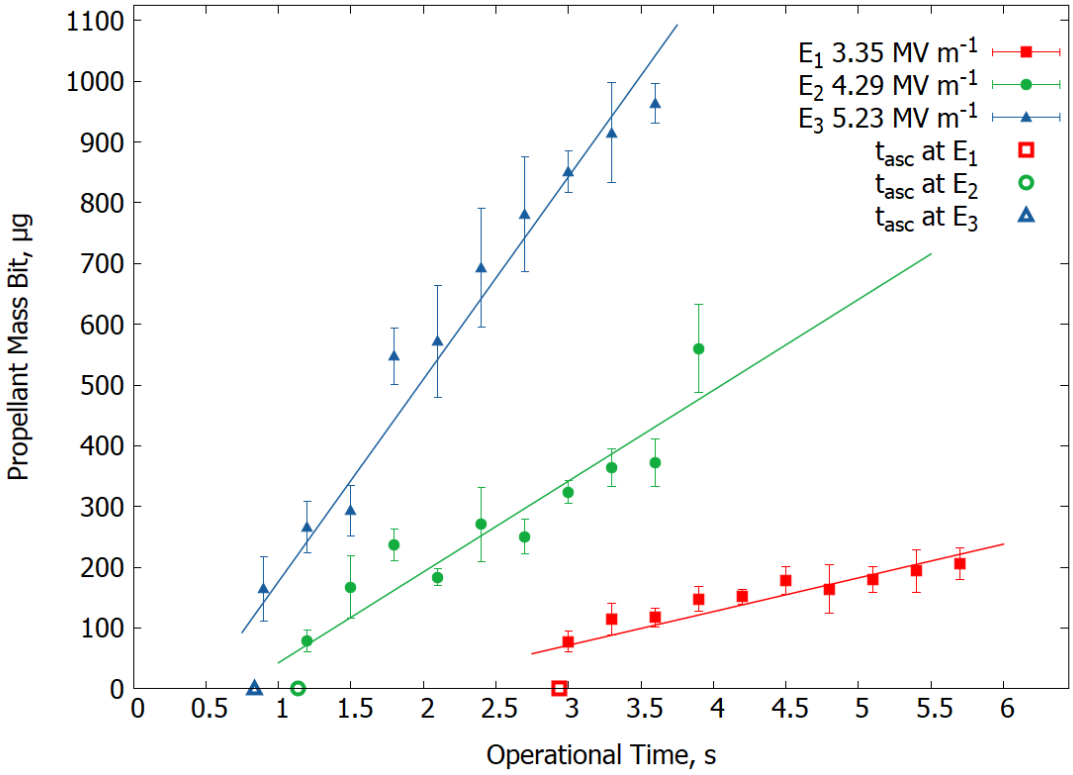

Figure 3. Results of the EFF unit operating with PFPE as propellant. Three electric fields have been tested; the trends represent linear fittings of each data set. The hollow markers give t_{asc}, the experimentally observed ascending time, which corresponds to zero mass bit.

The data presented in Fig. (3) demonstrates the mass bit capabilities of the feeding unit. The mass bit increase with electric field is evident; as predicted by Eq. (7), the pressure increases with the applied electric field. Since the electrode geometry is maintained constant for all experiments, the pressure is controlled solely by voltage variation.

D. Model Validation

Three electric field values are employed in the experiment, E_1=3.35 MV m^{-1}, E_2=4.29 MV m^{-1} and E_3=5.23 MV m^{-1} for which the corresponding values for the ascending time are 2.94 s, 1.14 s and 0.84 s. Using the theoretically derived expression for the ascending time, namely Eq. (12), the predicted values

of the ascending time are 3.33 s, 1.33 s and 0.76 s, respectively. Taking into account limitations of the Hagen-Pouiseuille model applied to this dynamic process the ascending time is found to be in good agreement with the experimental observations, since the relative deviation of the predicted value to the experimentally obtained value are 12%, 15% and 10%, respectively.

However, when attempting to extrapolate the model to predict the mass flow rate obtained due to spreading (t_{spr}), the mass values are significantly overestimated.It was found the mass bit delivered is not proportional to E^2 as suggested by Eqs. (10) and (13). Clearly, the proposed simplifications to the flow model do not account for a range of phenomena taking place while the liquid spreads over the surface of the discharge chamber. To obtain an accurate prediction of the mass bit the transition of the conduit flow to discharge chamber flow would have to considered, e.g. via modelling the surface tension effects in thin films.

IV. Discussion and Analysis

In spite of limited applicability of the simplified theory, some semi-empirical relations can be drawn. Performing linear regression on the data reported in Fig. (3) returns values of 0.93, 0.87 and 0.97, respectively for E_1, E_2 and E_3. The strong linear dependence between the mass bit and operational time demonstrates the active feeding capabilities and the potential of continuous mass flow rate achievable with the EFF pump, which is confirmed by visual observations.

The ascending time of the liquid column is well predicted. However, since the mass bit delivered is above expected requirements and is not well predicted by the model, it is suggested to adjust the firing frequency, such that the ascending time is synchronized with the spark plug ignition instant. This will eliminate any liquid spreading/overflowing inside the discharge chamber. The ascending time is thus used to scale the feeding unit and the thruster operating frequency. Based on ablative PPTs operating at the same energy shot the mass bit can be assumed to be 10 μg, and for a hemispherical droplet at the top of the feeding conduit, the radius of the conduit is thus 0.11 mm. The length of the conduit is calculated via the aspect ratio, using Fig. (4), yielding 0.98 mm. Therefore, a mass bit in the range of interest for micro-PPTs can be achieved, and additionally, the traditional operational frequency of 1 Hz is not compromised. Previous investigations of the propellant bar thermal profile suggest that the length of the feeding conduit should not be shorter than 1 mm[23] (if the thermal conductivity of the ceramic is comparable to the one of Teflon) as not to increase the temperature of the PFPE residing in the tank. For a conduit radius of 0.11 mm, the conduit length required for 1 Hz thrusting frequency is 0.99 mm, at a pressure of 164 Pa.

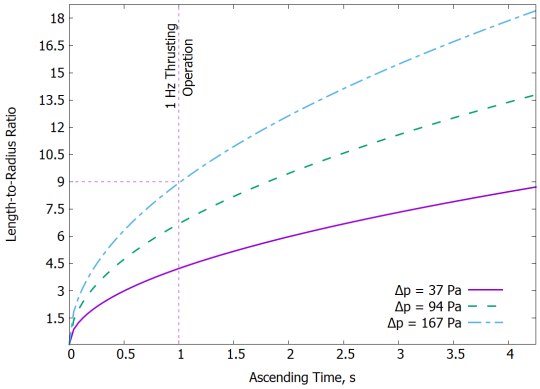

Figure 4. Conduit radius as a function of mass bit for the three electric pressure values tested, using L_c=3 mm, based on the simplified model of Sec. II.

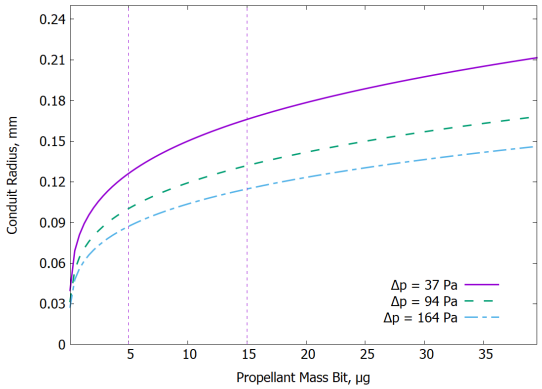

Figure 5. Length-to-radius dependence on ascending time (t_{asc}) for the three electric pressure values tested, based on the simplified model of Sec. II.

The operation of PPTs is discretized in pulses, allowing the engine to deliver a spectrum of thrust by electrically varying the discharge energy. By employing this method to modulate the thrust, mass bit is inefficiently accelerated as the increase in energy results in heat and post-ablation effects rather than electromagnetic acceleration.[24] Thus, the energy shot cannot optimally dose the mass bit and vary the thrust. For breech-fed thrusters a strong correlation has been found between the m_{bit}-to-E_{shot} ratio and the latent heat of vaporization, thermal conductivity of the layer and the layer thickness.[24] Thus, controlling

the ablated mass bit leads to thrust modulation. Moreover, as capacitors de-rate during extended operation, the m_{bit}-to-E_{shot} ratio can be optimally maintained using an active feeding system, leading to increased performance and reliability of μPPTs. It is noteworthy that PFPE has lower heat of vaporization compared to Teflon. This results in a decrease in the heat flux necessary to vaporize the propellant and hence more energy is available for ionizing and accelerating the neutral gas.

Present drawbacks of the feeding unit are the additional voltage signal required for the feeding electrode, and time delay between initiating the feeding system and the spark plug. Firstly, in these experiments a dedicated HV power supply is used for the feeding electrode. However, an easier method of applying the potential to the feeding electrode, as well as the spark plug, can be achieved via different voltage rising times; supplying the same voltage signal to both feeding electrode and spark plug, with a current-limiting resistor in series only with the spark plug, this will increase the voltage rising time on the spark plug. The resulting voltage waveform is qualitatively shown in Fig. (6), the value of the current-limiting resistor is then calculated using the propellant ascending time and time constants (τ), as per Eq. (14). Secondly, the operational time delay of the thruster introduced by the ascending time, t_{asc} is an intrinsic problem of any fluid propelled engine. As shown in Fig. (4), the propellant ascending time is proportional to the aspect ratio of the feeding conduit and thus the operating frequency of the thruster can be modulated, thus the time delay does not imply a practical limitations from a system operation viewpoint.

$$\tau_{ig} = \tau_{feed} + t_{asc} \tag{14}$$

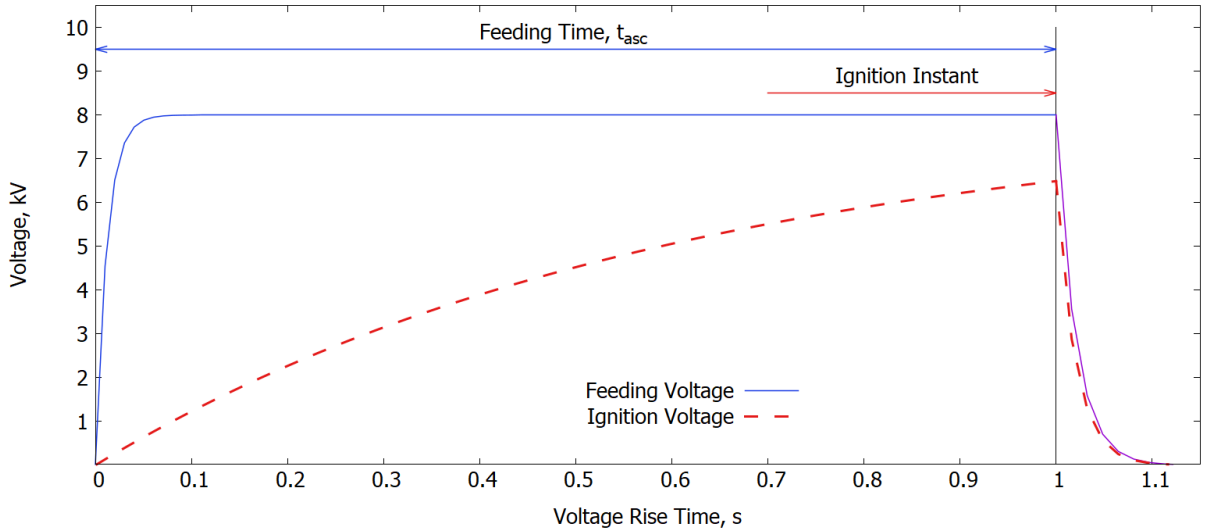

Figure 6. Qualitative timing diagram of feeding-to-ignition synchronization. The rise time of the ignition voltage is increased via a resistor, thus creating a delay of the rise time between the feeding voltage and ignition instant. This eliminates the need of an additional voltage signal for the feeding electrode.

The linearity observed in the mass flow rate extends the application of the electrostatic pump. A continuous mass flow rate may be desired for continuous thrust operation, particularly in a HFB mode. This operational mode has been demonstrated to increase Isp and to lower the LTA effects for both solid[8] and gas[25] fed PPTs. Moreover, high discharge energy PPTs require a significantly larger mass bit, e.g. mbit = 2 mg combined with E_{shot} = 6kJ would deliver Ibit = 100 mNs under Isp = 5000 s.[26] Our electrostatic pump can deliver similar propellant masses per shot, the experimental results show an achievable mass bit of 0.96 $\pm$ 0.03 mg. Scaling up, based on published results,[25] it is expected that coaxial LPPT with mbit = 0.2 mg combined with E_{shot} = 5 kJ would deliver Ibit = 32 mNs under Isp = 16000 s, offering significant savings of propellant. Of course, proposed electrostatic pump for LPPT (and controllable mbit) allows a variation in thrust without compromising efficiency and propellant utilization. Such high-energy thrusters are applicable for low-cost deep-space missions, e.g. lunar mission for small 10-20 kg spacecrafts.[27,28]

V. Future Work

The planned work involves a comprehensive sensitivity study, based on modelling and experimental efforts, to identify the optimum physical dimensions of the feeding line, such as radius and length, targeting propellant delivery of 5-10 micrograms. The optimised EFF unit will consequently be manufactured to test the effects of a new conduit and conclude on the applicability of this technology for liquid pulsed plasma thrusters.

Further, the LPPT prototype presently in development will soon be finalized, incorporating the optimised feeding unit. The LPPT prototype will offer variable mass bit and explore the performance achievable, focusing on the investigation of LTA effects. Using time-resolved current-voltage measurements, thrust measurements and optical spectroscopy techniques, an investigation into the optimal m_{bit}-to-E_{shot} ratio will be undertaken.

VI. Conclusion

According to the fundamental formula for electric force density in dielectric liquids, an expression of the electric pressure has been derived and employed to generate pumping forces inside a custom-made test cell. Consequently, a liquid feeding unit has been built and tested, thus demonstrating proof-of-concept of the novel EFF unit. The active feeding sub-system consists of no moving parts and minimum derivations from the traditional device are needed to operate the pump. The electrostrictive force-feeding unit demonstrates stable operation at three different electric fields, where the mass bit increases with applied voltage, and continuous mass flow rate capabilities are demonstrated. The minimum mass bit delivered by the EFF unit is 77.22 μg, and given the semi-empirical relations derived from the fundamental theory a mass bit reduction targeting 5 - 10 μg range is shown to be feasible, for which the design parameters of the pump are given.

The benefits of an EFF unit on-board a liquid-fed PPT are the active and discretized mass bit delivery capabilities, and electronic control of the flow rate. Moreover, the unit is easy to implement due to its inherent simplicity and low cost. It is conjectured that a discretized mass bit of variable size will significantly decrease, or eliminate LTA effects, consequently increasing PPT performance and market appeal.

Acknowledgments

The authors would like to thank the Tony Davis High Voltage Laboratory staff for their help during the experimental stage of the work and the UK Engineering and Physical Sciences Research Council (EPSRC) for the funding allocated towards this project. In addition, C. Dobranszki would like to thank the European project PATH (H2020-MSCA-RISE-2016-734629) for the insightful knowledge regarding plasma technologies. Paolo Gessini, in particular, wishes to thank the Brazilian Federal District Research Support Foundation, FAPDF, for the funding that allowed him to attend the 36th International Electric Propulsion Conference (IEPC 2019), contribute to this paper and present another one.

References

[1]Guarducci, F., Coletti, M., and Gabriel, S. B., "Design and Testing of a Micro Pulsed Plasma Thruster for Cubesat Application" *32nd International Electric Propulsion Conference*, IEPC-2011-239, Wiesbaden, DE, 2013.

[2]Dankanich, J. W., "Small Satellite Propulsion," NASA, Rept. M15-4339, Marshall Space Flight Center, Jan. 2015.

[3]Burton, R. L., and Turchi, P. J., "Pulsed Plasma Thruster," *J. of Propulsion and Power*, Vol. 14, No. 5, 1998.

[4]Vondra, R. J., Thomassen, K., and Solbes, A., "Analysis of Solid Teflon Pulsed Plasma Thruster," *J. of Spacecraft and Rockets*, Vol. 7, No. 12, 1970, pp. 1402-1406.

[5]Eckman, R., Gatsonis, N. A., Myers, R. M. and Pencil, E. J., "Experimental Investigation of the LES 8/9 Pulsed Plasma Thruster Plume," *25th International Electric Propulsion Conference*, IEPC-1997-126, Cleveland, OH, 1997, pp. 797-802.

[6]Marques, R. I., Gabriel, S. B., and de Souza Costa, F. "Progress on the Design of a Double Discharge Pulsed Plasma Thruster for the UniSat-5 Satellite," *44th AIAA/ASME/SAE/ASEE Joint Propulsion Conference and Exhibit*, Hartford, CT, 2008.

[7]Spanjers, G. G., Lotspeich, J. S., McFall, K. A., and Spores, R. A., "Propellant Losses Because of Particulate Emission in a Pulsed Plasma Thruster" *J. of Propulsion and Power*, Vol. 14, No. 4, 1998, pp. 554-559.

[8]Marques, R. I., Gabriel, S. B., and de Souza Costa, F. "Preliminary Results of a High Frequency Pulsed Plasma Thruster," *43rd AIAA/ASME/SAE/ASEE Joint Propulsion Conference and Exhibit*, Cincinnati, OH, 2007.

[9]Marques, R. I., Gabriel, S. B., and de Souza Costa, F. "The Two-Stage Pulsed Plasma Thruster," *31st International*

Electric Propulsion Conference IEPC-2009-250, Ann Arbor, MI, 2009.

[10]Kakami, A., Koizumi, H., Komurasaki, K., and Arakawab, Y., "Design and Performance of Liquid Propellant Pulsed Plasma Thruster," *Vacuum*, Vol. 73, Apr., 2004, pp. 419-425.

[11]Koizumi, H., Kawazoe, Y., Komurasaki, K., and Arakawa, Y., "Effect of Solute Mixing in the Liquid Propellant of a Pulsed Plasma Thruster," *Vacuum*, Vol. 80, Sep., 2006, pp. 1234-1238.

[12]Schönherr, T., Abe, Y., Okamura, K., Koizumi, H., Arakawa, Y., and Komurasaki, K., "Influence of Propellant in the Discharge Process of PPT," *48th AIAA/ASME/SAE/ASEE Joint Propulsion Conference and Exhibit*, Atlanta, GA, 2012.

[13]Barral, S., Kurzyna, J., Remírez, E., Martín, R., Ortiz, P., et al., "Development Status of an Open Capillary Pulsed Plasma Thruster with Non-Volatile Liquid Propellant" *33rd International Electric Propulsion Conference*, IEPC-2013-291, Washington, DC, 2013.

[14]Patel, A. R., Zhang, Y., and Shashurin, A., "Liquid-Fed Pulsed Plasma Thruster for Propelling Nanosatellites," *J. of Physics D: Applied Physics*, arXiv:1907.00169v1 (submitted June 2019).

[15]Scharleman, C., "Investigation of Thrust Mechanisms in a Water Fed Pulsed Plasma Thruster," PhD. Dissertation, Aeronautical and Astronautical Engineering, Ohio State Univ., OH, 2003.

[16]Ling, W. Y. L., Schönherr, T., and Koizumi, H., "Characteristics of a Non-Volatile Liquid Propellant in Liquid-fed Ablative Pulsed Plasma Thrusters," *J. of Applied Physics*, Vol. 121, No. 7, 2017, pp. 1-11.

[17]Stratton, J. A., *Electromagnetic Theroy*, 1st ed., McGraw-Hill Book Company, Inc., New York and London, 1941, Ch. 2, pp. 145-151.

[18]Landau, L. D., and Lifshitz, E. M., *Electrodynamics of Continuous Media (Volume 8)*, 2nd ed., Course of Theoretical Physics - Series, Pergamon Press, Oxford, 1984, Ch. 2, 15, page 62.

[19]Jones, T. B., "On the Relationship of Dielectrophoresis and Electrowetting," *Langmuir*, Vol. 18, No. 11, 2002, pp. 4437-4443.

[20]Ushakov, V. Y., Klimkin, V. F., and Korobeynikov, S. M., *Impulse Breakdown of Liquids*, 1st ed., Springer-Verlag Berlin Heidelberg, New York, 2007, Ch. 1, page 3.

[21]Dobranszki, C., Golosnoy, I. O., and Gabriel, S. B., "Development of Ignition Unit for a Liquid Pulsed Plasma Thruster," *6th Space Propulsion Conference*, SP2018_117, Seville, SP, 2018.

[22]Landau, L. D., and Lifshitz, E. M., *Fluid Mechanics (Volume 2)*, 2nd ed., Course of Theoretical Physics - Series, Pergamon Press, Oxford, 19, Ch. 2, 17, page 53, 58.

[23]Spanjers, G. G., Malak, J. B., Leiweke, R. J., and Spores, R. A., "Effect of Propellant Temperature of Efficiency in the Pulsed Plasma Thruster" *J. of Propulsion and Power*, Vol. 14, No. 4, 1998, pp. 545-553.

[24]Solbes, A., and Vondra, R. J., "Performance Study of a Solid Fuel-Pulsed Electric Microthruster" *J. of Spacecraft and Rockets*, Vol. 10, No. 6, 1972, pp. 406-410.

[25]Ziemer, J. K., Cubbin, E. A., Choueiri, E. Y., and Brix, D., "Performance Characterization of a High E±ciency Gas-Fed Pulsed Plasma Thruster" *33rd Joint Propulsion Conference and Exhibit*, Seattle, WA, 1997.

[26]Kazeev, M. N., and Kozlov, V. F., "Ablation-Fed Discharge Characteristics" *31st International Electric Propulsion Conference*, IEPC-2009-249, Ann Arbor, MI, 2009.

[27]Gessini, P., Marques, R. I., Cas, P. L. K. da, Vendittozzi, C., Santilli, G., Possa, G. C., Ferreira, J. L., Habl, L. T. C., Gabriel, S. B., "SmallSat High-Energy Missions Using Ablative Pulsed Plasma Thrusters," *3rd IAA LACW - 3rd IAA Latin American CubeSat Workshop*, Ubatuba, BR, 2018.

[28]Gessini, P., Possa, G. C., Marques, R. I., Dobranszki, C., Golosnoy, I. O., and Gabriel, S. B., "Enabling High-Energy Missions with Small Spacecraft by Using Pulsed Plasma Thrusters", *36th International Electric Propulsion Conference*, IEPC-2019-815, Vienna, AT, 2019.